Inorg. Chem. **2008**, *47*, 9797−9803

Trianionic Organoborate Triangles

Brendan F. Abrahams,* Berin A. Boughton, Haozhen Choy, Oliver Clarke, Martin J. Grannas, David J. Price, and Richard Robson*

School of Chemistry, University of Melbourne, Victoria 3010, Australia

Received March 27, 2008

The rigid, angular ligand 3,3,3′,3′-tetramethyl-1,1′spirobisindane-5,5′,6,6′-tetrol, LH_4, in the form of its tetra-anion, L^{4-}, affords crystalline compounds containing the triangular macrocyclic boron derivative $[B_3L_3]^{3-}$ with the counter cations, triethylammonium, imidazolium, tetraethylammonium, and protonated dabco (dabco = 1,4-diazabicyclo[2,2,2]octane). Within a triangular unit all three chiral L^{4-} ligands have the same hand although the crystal does contain a racemic mixture of macrocycles. In all four compounds, one out of the three counter-cations per macrocycle is bound inside the macrocycle.

Introduction

Multifunctional catechol-based ligands have been extensively employed in a variety of supramolecular systems.[1] The double negative charge associated with the deprotonated catecholate unit as well as the ligand's ability to chelate means that it can bind both strongly and in a predictable manner to a range of metal centers. The use of such multifunctional ligands in supramolecular systems is not confined to metal-based systems. It was reported recently that the ligand 3,3,3′,3′-tetramethyl-1,1′spirobisindane-5,5′,6,6′-tetrol (**1**; hereafter LH_4), after deprotonation to give the tetra-anion L^{4-}, affords macrocyclic boron derivatives, $[B_4L_4]^{4-}$, with the square arrangement shown in Figure 1.[2] A number of derivatives of this anionic macrocycle with a variety of counter-cations have now been isolated. A structural feature common to all of these compounds is that the $[B_4L_4]^{4-}$ squares are stacked one on top of another, glued together electrostatically by cations located generally above and below the anionic boron centers. The columns generated in this way resemble tubes with a void of roughly square cross-section and of roughly nanometer dimensions running down the center (Supporting Information, Figure S1).

1 is an angular and relatively rigid molecule with its two catechol units constrained to remain in an approximately fixed geometrical relationship to one another; this structural feature is responsible for some of the stereochemical aspects discussed below. **1** is a chiral molecule; the readily available racemic mixture was used to generate the $[B_4L_4]^{4-}$ compounds above and also the derivatives reported below. All four L^{4-} components within a $[B_4L_4]^{4-}$ square are of the same hand. With certain counter-cations all the squares in a column are of the same hand, whereas with other cations the squares within a column alternate in hand.[2] In continuation of our work with the boron derivatives of L^{4-} we report here some derivatives of the new triangular $[B_3L_3]^{3-}$ macrocycle, in which, again, the "twist" at each boron connection allows all three ligands to have the same hand within a single macrocycle although each of the crystals consists of a racemic mixture of triangular $[B_3L_3]^{3-}$ anions.

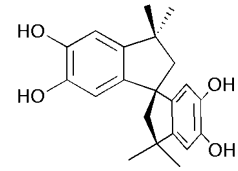

1

Experimental Section

Solvated $(Et_3NH)_3[B_3L_3]$. A solution of $B(OMe)_3$ (0.200 g, 1.92 mmol) in methanol (1 mL) was added to a stirred suspension of LH_4 (0.682 g, 2.00 mmol) in methanol (2 mL) containing triethylamine (1 mL) at room temperature (RT), upon which the LH_4 rapidly dissolved. After 2 weeks a colorless crystalline solid separated, consisting of small triangular crystals. The solid was collected, washed with methanol and dried in air. Yield, 0.705 g (96%). Anal. (%): Found: C, 68.7; H, 7.7; N, 3.1. Calcd for $(Et_3NH)_3[B_3L_3]\cdot 4H_2O$ ($C_{81}H_{120}B_3N_3O_{16}$): C, 68.5; H, 8.2; N, 3.0. The X-ray powder diffraction pattern of the bulk material matched that calculated from the crystal structure. ^{1}H NMR (400 MHz, DMSO-d_6, rt): δH (ppm) 6.27 (s, 6H, Ar), 5.61 (s, 6H, Ar), 2.99

* To whom correspondence should be addressed. E-mail: bfa@unimelb.edu.au (B.F.A.), r.robson@unimelb.edu.au (R.R.).

10.1021/ic800544j CCC: $40.75
Published on Web 10/01/2008

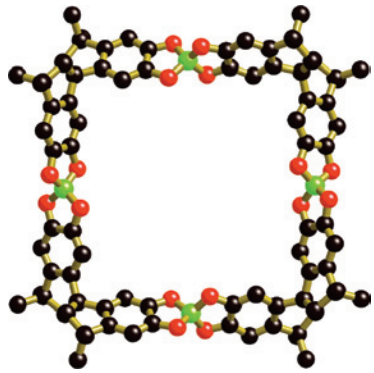

Figure 1. $[B_4L_4]^{4-}$ macrocycle. Boron centers can be seen located somewhat "outside" the imaginary square formed by linking the spiro carbon centers together. Hydrogen atoms have been omitted for clarity. Color code: O, red; C, black; B, green.

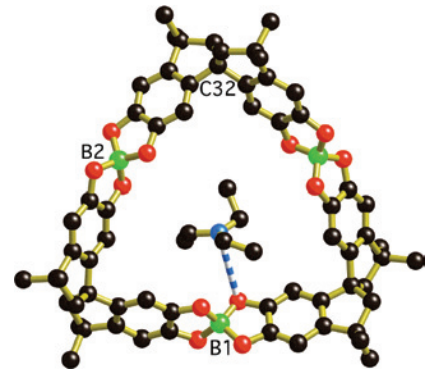

Figure 2. $[B_3L_3]^{3-}$ component of solvated $(Et_3NH)_3[B_3L_3]$ showing the intra-triangle cation. Blue and white striped connections represent hydrogen bonds. Hydrogen atoms have been omitted for clarity. Color code: O, red; N, blue; C, black; B, green.

(q, ^3J 7.2 Hz, 18H, -CH_2- of Et_3NH), 2.23 (d, ^2J 12.6 Hz, 6H, -CH_2- of L), 1.92 (d, ^2J 12.6 Hz, 6H, -CH_2- of L), 1.25 (s, 36H, -CH_3 of L), 1.06 (t, ^3J 7.2 Hz, 27H, -CH_3 of Et_3NH). IR (KBr disk, cm^{-1}): 3435mbr, 3024m, 2950s, 2859s, 2731m, 2562w, 1610m, 1482s, 1392m, 1359m, 1305m, 1272s, 1225s, 1197s, 1076s, 929ssh, 903s, 855s, 815m, 738m, 714m, 691s, 669vw, 601vw, 576vw, 552w, 527vw, 503vw, 481vw, 459vw, 420vw.

Solvated $(C_3H_5N_2)_3[B_3L_3]$. A solution of $B(OMe)_3$ (0.399 g, 3.84 mmol) in acetonitrile (1 mL) was added to a stirred, refluxing suspension of LH_4 (1.363 g, 4.00 mmol) and imidazole (0.601 g, 8.83 mmol) in acetonitrile (40 mL), resulting in immediate dissolution of all solid. Within seconds an off-white precipitate formed. After the mixture had been allowed to cool to RT the solid was collected, washed with acetonitrile, and dried in air. Yield 1.64 g. Anal. (%): Found: C, 65.5; H, 6.1; N, 8.0. Calcd for $(C_3H_5N_2)_3[B_3L_3]\cdot 2MeCN\cdot 3.5H_2O$ ($C_{76}H_{88}B_3N_8O_{15.5}$): C, 65.5; H, 6.4; N, 8.0. ^{1}H NMR (400 MHz, DMSO-d_6, rt): δH (ppm) 8.66 (s, 3H, Ar of Himid), 7.44 (s, 6H, Ar of Himid), 6.29 (s, 6H, Ar of L) 5.64 (s, 6H, Ar of L), 2.23 (d, ^2J 12.6 Hz, 6H, -CH_2- of L), 1.92 (d, ^2J 12.6 Hz, 6H, -CH_2- of L), 1.26 (s, 36H, -CH_3 of L). IR (KBr disk, cm^{-1}): 3436mbr, 3149s, 2952s, 2860s, 2651m, 1596m, 1482s, 1361m, 1306m, 1273s, 1225m, 1198m, 1080s, 996vw, 931m, 879m, 860m, 820w, 751w, 740w, 713vw, 692w, 669vw, 659vw, 630w, 602vw, 553vw, 527vw, 501vw, 482vw. Crystals suitable for single crystal X-ray diffraction study were obtained from a more dilute reaction mixture, when a solution containing $B(OMe)_3$ (30 mg, 0.3 mmol), LH_4 (90 mg, 0.3 mmol), and imidazole (40 mg, 0.5 mmol) in boiling acetonitrile (50 mL) was allowed to cool.

Solvated $(Et_4N)_3[B_3L_3]$. Crystals suitable for single-crystal X-ray diffraction were obtained directly from a solution containing $B(OMe)_3$ (0.03 g, 0.3 mmol) and LH_4 (0.09 g, 0.3 mmol) in a methanolic solution of Et_4NOH (1 mL, 25% solution) heated at 150 °C in a sealed tube for 4 days. The crystals were collected and dried in air. The X-ray powder diffraction pattern of the bulk material matched that calculated from the crystal structure. Elemental Analysis (%): Found: C, 65.4; H, 8.4; N, 2.7. Calcd for $(Et_4N)_3[B_3L_3]\cdot 9H_2O$ ($C_{87}H_{138}B_3N_6O_{21}$): C, 65.5; H, 8.4; N, 2.6. ^{1}H NMR (400 MHz, DMSO-d_6, rt): δH (ppm) 6.26 (s, 6H, Ar of L) 5.58 (s, 6H, Ar of L), 3.14 (q, ^3J 7.2 Hz, 24H, -CH_2- of NEt_4), 2.23 (d, ^2J 11.4 Hz, 6H, -CH_2- of L), 1.92 (d, ^2J 11.4 Hz, 6H, -CH_2- of L), 1.23 (s, 36H, -CH_3 of L), 1.06 (t, ^3J 7.2 Hz, 36H -CH_3 of NEt_4). Infrared spectrum (KBr disk, cm^{-1}): 3450 mbr, 2951s, 2859m, 1483s, 1394w, 1304w, 1271s, 1226m, 1197m, 1107s, 1074s, 906m, 855w, 786vw, 738w, 714w, 692w,

Solvated $(dabcoH)_3[B_3L_3]$. A solution of $B(OMe)_3$ (0.407 g, 3.92 mmol) in methanol (0.5 mL) was added to a stirred refluxing suspension of LH_4 (1.354 g, 3.98 mmol) and dabco (0.940 g, 8.38 mmol) in a mixture of *n*-PrOH (5 mL) and MeOH (1 mL). Within seconds all the solid had dissolved. After approximately 20 min an off-white precipitate had formed. The mixture was allowed to cool to RT and the solid was collected, washed with *n*-PrOH/MeOH and dried in air. Yield 1.142 g (73%). Elemental Analysis (%): Found: C, 66.2; H, 7.7; N, 5.5. Calcd for $(dabcoH)_3[B_3L_3]\cdot 3n\text{-}PrOH\cdot 2H_2O$ ($C_{90}H_{133}B_3N_6O_{17}$): C, 66.3; H, 8.4; N, 5.2. The X-ray powder diffraction pattern of the bulk material matched that calculated from the crystal structure. ^{1}H NMR (400 MHz, DMSO-

Table 1. Crystallographic Data

compound	$(HNEt_3)_3B_3L_3\cdot 1.5MeOH$	$(C_3N_2H_5)_3B_3L_3\cdot 7MeCN$	$(NEt_4)_3B_3L_3\cdot 2MeOH$	$(N_2C_6H_{13})_3B_3L_3\cdot 4PrOH\cdot H_2O$
formula	$C_{82.5}H_{114}B_3N_3O_{13.5}$	$C_{86}H_{96}B_3N_{13}O_{12}$	$C_{89}H_{128}B_3N_3O_{14}$	$C_{93}H_{133}B_3N_3O_{17}$
M	1396.20	1536.19	1496.37	1639.48
crystal system	monoclinic	monoclinic	triclinic	triclinic
space group	$C2/c$	$C2/c$	$P\bar{1}$	$P\bar{1}$
a/Å	20.343(3)	18.122(13)	14.6309(9)	15.743(2)
b/Å	29.068(4)	29.69(2)	17.7050(10)	17.385(2)
c/Å	13.680(2)	15.313(11)	18.1066(9)	18.338(2)
α/deg	90	90	112.696(5)	111.261(2)
β/deg	91.177(2)	94.10(1)	91.910(5)	100.393(2)
γ/deg	90	90	92.831(5)	93.644(2)
V/Å^3	8088(2)	8217(10)	4314.9(4)	4554.8(8)
Z	4	4	2	2
μ/mm^{-1}	0.076	0.083	0.602	0.081
unique reflections	7122	9191	11631	19820
R_{int}	0.0666	0.1951	0.0552	0.0655
reflections ($I > 2\sigma(I)$)	3520	2221	8316	6744
wR_2 (all data)	0.3681	0.3053	0.4777	0.2254
R_1 [$I > 2\sigma(I)$]	0.1132	0.0944	0.1462	0.0891

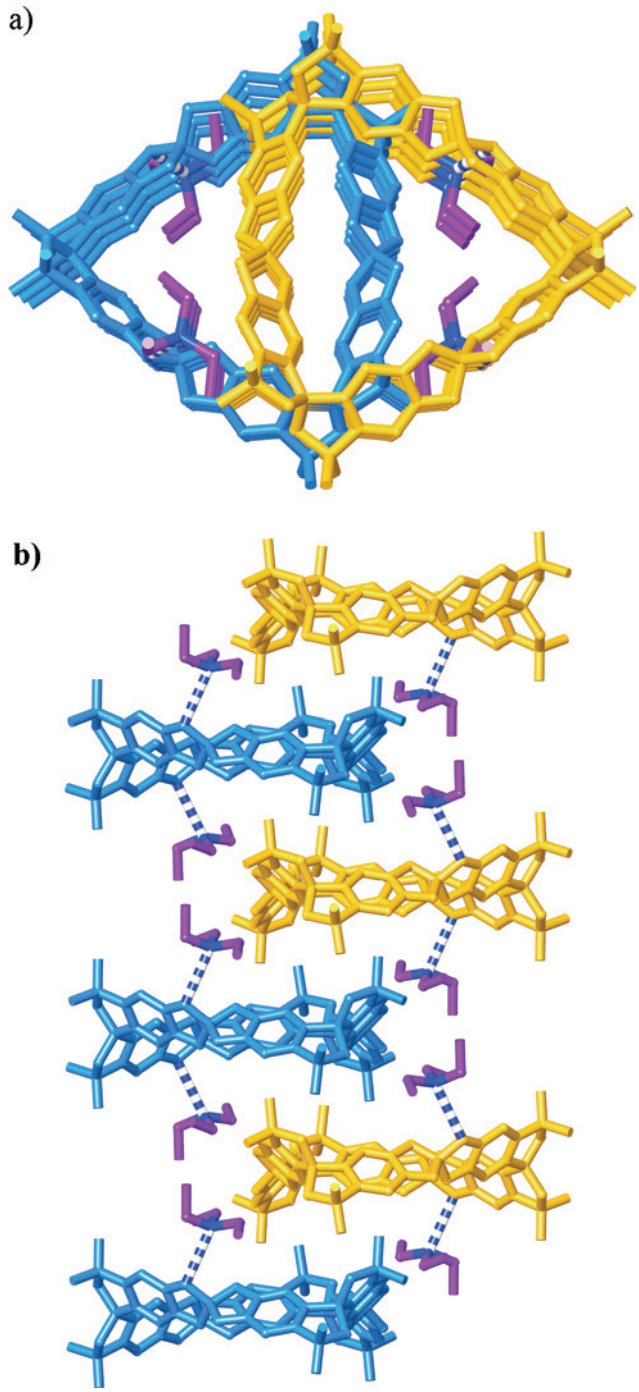

Figure 3. Stacking mode of the chiral $[B_3L_3]^{3-}$ triangular units in solvated $(Et_3NH)_3[B_3L_3]$. Triangles alternate in hand; the two enantiomers are shown here in gold and blue. The intra-triangle cations are omitted here for clarity. The view in 3a is looking down the stacking direction; that in 3b is "side-on" to the stacking direction. Blue and white striped connections represent hydrogen bonds. Hydrogen atoms have been omitted for clarity.

d_6, rt): δH (ppm) 6.30 (s, 6H, Ar of L), 5.52 (s, 6H, Ar of L), 2.913 (s, 36H, -CH_2- of dabcoH), 2.24 (d, ^2J 12.6 Hz, 6H, -CH_2- of L), 1.93 (d, ^2J 12.4 Hz, 6H, -CH_2- of L), 1.25 (s, 36H, -CH_3 of L). Infrared spectrum (KBr disk, cm^{-1}): 3400mbr, 3022w, 2952s, 2860m, 2642w, 1630w, 1482s, 1363w, 1321w, 1305w, 1272s, 1219m, 1198m, 1078s, 901m, 862m, 785vw, 739w, 714w, 693w, 670vw, 602w, 552vw, 481vw. Crystals suitable for single-crystal X-ray diffraction studies were obtained upon cooling an initially boiling solution of $B(OMe)_3$ (0.054 g, 0.52 mmol), LH_4 (0.18 g, 0.52 mmol), and dabco (0.23 g, 2.1 mmol) in methanol (1 mL) and *n*-PrOH (4 mL).

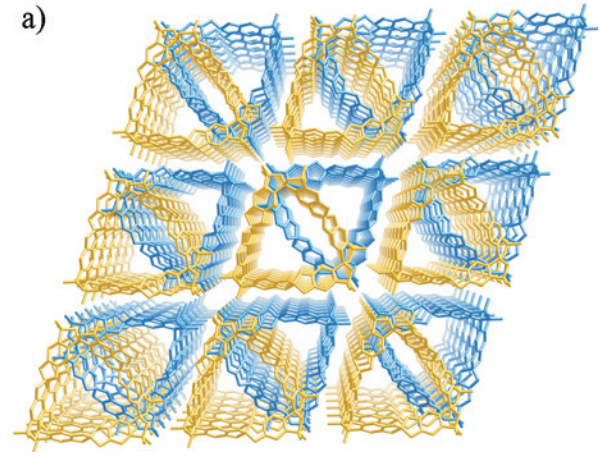

Figure 4. Packing of the columns in solvated $(Et_3NH)_3[B_3L_3]$. The two different types of enantiomer are shown in gold and blue. Hydrogen atoms have been omitted for clarity.

Crystallography

The crystals described in this work are very poorly diffracting, a result of the relatively large amounts of disordered solvent and the fact that the heaviest atom in the crystals is oxygen. As a consequence, the agreement values reported are somewhat elevated. Despite the difficulties in modeling disordered species within the crystals, the atomic positions of the non-hydrogen atoms within the anionic triangles are very clearly defined. Similarly, the atomic positions in the cation are also well-defined although in some cases it was necessary to model the cation over two sites. The particularly poor agreement values obtained for the NEt_4^+ crystals is a consequence of severe twinning which adversely affected the quality of the diffraction data.

Data for the $NHEt_3^+$, $C_3N_2H_5^+$, and $dabcoH^+$ compounds were measured on a Bruker CCD diffractometer fitted with graphite monochromated Mo Kα radiation ($\lambda = 0.71073$ Å). An Oxford Xcalibur CCD diffractometer fitted with Cu Kα radiation ($\lambda = 1.54184$ Å) was used to collect data on the NEt_4^+ crystal. Structures were solved using direct methods and refined using a full matrix least-squares procedure based on F^2 (SHELX-97).[3] Crystallographic data are presented in Table 1.

(1) (a) Albrecht, M.; Janser, I.; Frohlich, R. *Chem. Commun.* **2005**, *2*, 157–165. (b) Albrecht, M. *Chem. Soc. Rev.* **1998**, *27* (4), 281–288. (c) Pierpont, C. G.; Lange, C. W. *Prog. Inorg. Chem.* **1994**, *41*, 331–442. (d) Duhme, A. K. *J. Chem. Soc., Dalton Trans.* **1997**, 773. (e) Duhme, A. K.; Dauter, Z.; Hider, R. C.; Pohl, S. *Inorg. Chem.* **1996**, *35*, 3059. (f) Caulder, D. L.; Raymond, K. N. *J. Am. Chem. Soc.* **2001**, *123*, 8932. (g) Duhme-Klair, A. K.; Vollmer, G. *Angew. Chem., Int Ed.* **2000**, *39*, 1626. (h) Thuery, P.; Masci, B. *Supramol. Chem.* **2003**, *15* (2), 95. (i) Fiedler, D.; Pagliero, D.; Brumaghim, J. L.; Bergman, R. G.; Raymond, K. N. *Angew. Chem., Int. Ed.* **2006**, *43*, 846. (j) Leung, D. H.; Fiedler, D.; Raymond, K. N.; Bergman, R. G. *Angew. Chem., Int. Ed.* **2004**, *43*, 963. (k) Leung, D. H.; Fiedler, D.; Raymond, K. N.; Bergman, R. G. *J. Am. Chem. Soc.* **2004**, *126*, 3674. (l) Tiedermann, B. E. F.; Raymond, K. N. *Angew. Chem., Int. Ed.* **2006**, *45*, 83–86. (m) Caulder, D. L.; Power, R. E.; Parrac, T. N.; Raymond, K. N. *Angew. Chem., Int. Ed.* **1998**, *37*, 1840. (n) Whittle, B.; Everest, N. S.; Howard, C.; Ward, M. D. *Inorg. Chem.* **1995**, *34*, 2025. (o) Bajaj, H. C.; Das, A.; Shukla, A. D.; Whittle, B. *Inorg. Chim. Acta* **1998**, *267* (1), 1–5. (p) Pierpont, C. G.; Buchanan, R. M. *Coord. Chem. Rev.* **1981**, *38* (1), 45–87. (q) Abrahams, B. F.; FitzGerald, N. J.; Robson, R. *Angew. Chem., Int. Ed.* **2007**, *46*, 8640. (r) McCord, D. J.; Small, J. H.; Greaves, J.; Van, Q. N.; Shaka, A. J.; Fleischer, E. B.; Shea, K. J. *J. Am. Chem. Soc.* **1998**, *120*, 9763.

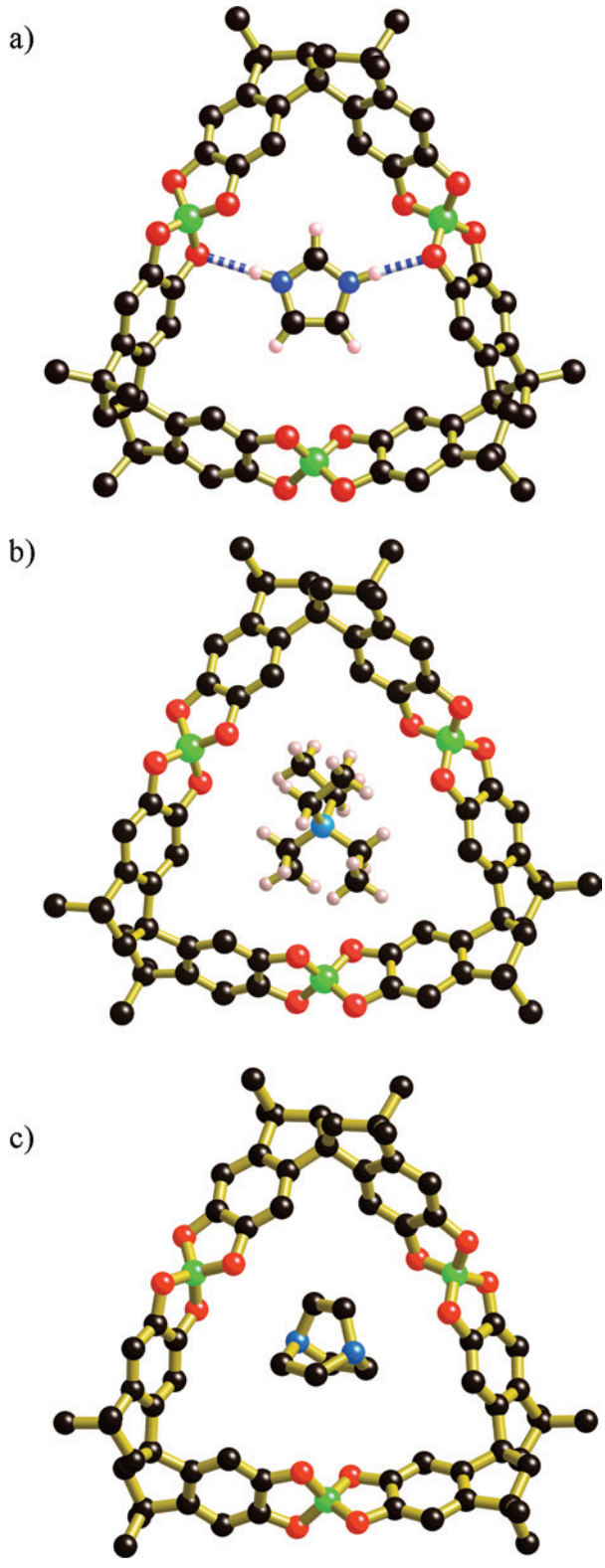

Figure 5. Representation of the $[B_3L_3]^{3-}$/intra-triangle cation association where (a) cation = $C_3H_5N_2^+$, (b) cation = Et_4N^+ and (c) cation = dabcoH$^+$. Some hydrogen atoms have been omitted for clarity. Color code: O, red; N, blue; C, black; B, green; H, pink.

Results and Discussion

When trimethylborate, LH_4, and triethylamine are combined in methanol, a solution is obtained which persists at room temperature without precipitating any solid for several days; if the solution is heated in a sealed tube to 160 °C,

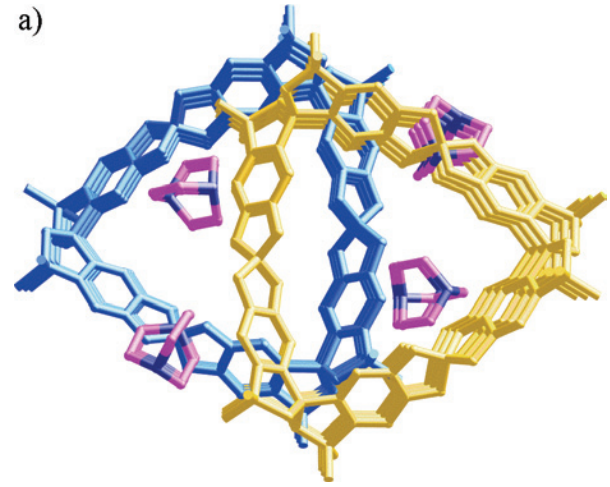

Figure 6. Representation of the hydrogen bonding chain in $(dabcoH)_3[B_3L_3].4PrOH\cdot H_2O$. The two different types of extra-triangle dabcoH$^+$ are shown. The two different types of enantiomer are shown in gold and blue. Hydrogen atoms have been omitted for clarity.

crystals of solvated $(Et_3NH)_4[B_4L_4]$ separate from the hot mixture.[2] We have now discovered that if the methanolic solution is left at room temperature in a capped vial for 2 or 3 weeks, crystals with a triangular outline are formed that are visibly different from the crystals of solvated $(Et_3NH)_4[B_4L_4]$. Single crystal X-ray diffraction indicates that the crystals formed at room temperature contain the 3:3 macrocycle, $[B_3L_3]^{3-}$. The macrocycle has a triangular appearance as can be seen in Figure 2, with the spiro carbon atoms providing the corners and with the catechol-B-catechol units forming the edges. There are two types of Et_3NH^+ cations in the structure. One type is located inside the triangle, as shown in Figure 2, and this is referred to as the intra-triangle cation, the other type being referred to as the extra-triangle cation. As in the $[B_4L_4]^{4-}$ squares, all the L^{4-} units within the triangular macrocycle have the same hand, a geometrical feature made possible again by the "twist" at each boron center referred to above. A 2-fold axis passes through one boron atom [B1 in Figure 2] and through the spiro carbon [C32 in Figure 2] belonging to the ligand not directly associated with B1 that is located at the opposite corner of the triangle. A Et_3NH^+ cation located inside the triangle is disordered around the 2-fold axis and forms a hydrogen bond with a catechol oxygen atom associated with B1 as indicated in Figure 2 (O···N 3.15(1) Å) which shows only one of the arrangements of the cation.

The triangular $\{[B_3L_3](Et_3NH)\}^{2-}$ composite anionic units form stacks, as represented in Figure 3, in which the chiral macrocycles alternate in hand. The blue macrocycles are all of the same hand and the gold macrocycles are of the opposite hand. The 2-fold axes of the triangles in a stack are all parallel and perpendicular to the stacking direction. The extra-triangle Et_3NH^+ cations are located with their nitrogen centers close to the B···B···B line that runs in the

(2) Abrahams, B. F.; Price, D. J.; Robson, R. *Angew. Chem., Int. Ed.* **2006**, *45*, 806.
(3) Sheldrick, G. M. *SHELX97 - Programs for Crystal Structure Analysis*, release 97−2; Institüt für Anorganische Chemie der Universität Göttingen: Göttingen, Germany, 1998.

Table 2. Reduced Cell Parameters

compound	$(HNEt_3)_3B_3L_3\cdot 1.5MeOH$	$(C_3N_2H_5)_3B_3L_3\cdot 7MeCN$	$(NEt_4)_3B_3L_3\cdot 2MeOH$	$(N_2C_6H_{13})_3B_3L_3\cdot 4PrOH\cdot H_2O$
a/Å	13.680(2)	15.313(11)	14.6309(9)	15.743(2)
b/Å	17.740(2)	17.392(11)	17.7050(10)	17.385(2)
c/Å	17.740(2)	17.392(11)	18.1066(9)	18.338(2)
α/deg	110.025(2)	117.20(1)	112.696(5)	111.261(2)
β/deg	90.682(2)	92.14(1)	91.910(5)	100.393(2)
γ/deg	90.682(2)	92.14(1)	92.831(5)	93.644(2)

Table 3. Major Ions Detected by ESI-MS in the Negative Ion Modes

compound	anions	exptl *m*/*z*	calcd *m*/*z*	error (ppm)	rel abund
$B_3L_3(HNEt_3)_3$	$[B_3L_3HNEt_3]^{2-}$	571.7817	571.7823	−1.1	100
	$[B_3L_3]^{3-}$	347.1439	347.1455	−4.6	24.3
	$[B_3L_3H]^{2-}$	521.2206	521.2218	−2.3	9.1
$B_3L_3(C_3N_2H_5)_3$	$[B_3L_3C_3N_2H_5]^{2-}$	555.2383	555.2408	−4.5	100
	$[B_3L_3]^{3-}$	347.1438	347.1455	−4.6	18.9
	$[B_3L_3Na]^{2-}$	532.2103	532.2128	−4.7	12.1
$B_3L_3(NEt_4)_3$	$[B_3L_3NEt_4]^{2-}$	585.7980	585.7972	−1.4	100
	$[B_3L_3]^{3-}$	347.1437	347.1455	−5.2	6.8
$B_3L_3(dabcoH)_3$	$[B_3L_3dabcoH]^{2-}$	555.2383	555.2408	−4.5	100
	$[B_3L_3]^{3-}$	347.1436	347.1455	−5.5	56.6
	$[B_3L_3H]^{2-}$	521.2202	521.2218	−3.1	29.5

stacking direction, displaced somewhat toward the "inside" of the stack, as can be seen in Figure 3a; two of the ethyl groups project toward the "outside" of the stack. The extra-triangle cations are hydrogen bonded to catechol oxygen atoms (O···N, 2.930(7) Å), as can be seen in Figure 3b. This mode of stacking of anionic macrocycles and extra-triangle Et_3NH^+ cations resembles that seen in solvated $(Et_3NH)_4[B_4L_4]$. In both cases, the overall electrically neutral $(Et_3NH)_n[B_nL_n]$ stack ($n = 3$ or 4) resembles a column with an essentially hydrophobic exterior surface, square in cross-section in the case of $(Et_3NH)_4[B_4L_4]$, and roughly rhombic in cross-section in the case of $(Et_3NH)_3[B_3L_3]$. Not surprisingly, the stacks in the two cases pack in a similar fashion, as can be seen in Figures 4 and S1. Of course, the channel running down the center of the stack in $(Et_3NH)_4[B_4L_4]$ is not present in the stack in $(Et_3NH)_3[B_3L_3]$.

In addition to solvated $(Et_3NH)_3[B_3L_3]$, we have discovered three other derivatives of the triangular $[B_3L_3]^{3-}$ ion, namely, those in which the counter cations are either imidazolium ($C_3H_5N_2^+$) or Et_4N^+ or dabcoH$^+$ (the protonated form of dabco, that is, 1,4-diazabicyclo[2,2,2]octane). Significantly, in these three cases, as in $(Et_3NH)_3[B_3L_3]$, one of the three counter cations per macrocycle is located inside the triangle.

Crystals of solvated $(C_3H_5N_2)_3[B_3L_3]$ are obtained from a reaction mixture containing trimethylborate, LH_4, and imidazole in refluxing acetonitrile; a methanolic reaction mixture containing trimethylborate, LH_4, and tetraethylammonium hydroxide in a sealed tube at 160 °C affords crystals of solvated $(Et_4N)_3[B_3L_3]$, and crystals of solvated $(dabcoH)_3[B_3L_3]$ are obtained from reaction mixtures in refluxing *n*-propanol/methanol containing trimethylborate, dabco, and LH_4. These three $[B_3L_3]^{3-}$ derivatives have been studied by single crystal X-ray diffraction. Figures 5a, 5b, and 5c show how the $C_3H_5N_2^+$, the Et_4N^+, and the dabcoH$^+$ intra-triangle cations, respectively, are located inside the $[B_3L_3]^{3-}$ macrocycle.

As with $(Et_3NH)_3[B_3L_3]$, a crystallographic 2-fold axis, passes through the B_3L_3 triangle in $(C_3H_5N_2)_3[B_3L_3]$. The planar imidazolium cation is located with its 2-fold axis coincident with that of the macrocycle and with its plane inclined by 9.9(6)° to the B_3 plane. It is hydrogen bonded on one side to a catechol oxygen center located above the B_3 plane and on the other side to an equivalent catechol oxygen center below the B_3 plane [N···O, 2.851(7) Å].

A similar arrangement of the B_3L_3 anion with the intra-triangle cation is apparent in $(Et_4N)_3[B_3L_3]$. In contrast to the Et_3NH^+ intra-triangle cation in solvated $(Et_3NH)_3[B_3L_3]$, the Et_4N^+ intra-triangle cation in solvated $(Et_4N)_3[B_3L_3]$ is ordered and is shown in Figure 5b. While there may appear to be a vertical 2-fold axis in Figure 5b, low symmetry crystal packing of the external cations results in the absence of crystallographic 2-fold symmetry. The C···O separations between certain carbon atoms of the Et_4N^+ cation and certain catechol oxygen atoms (3.34(1), 3.34(1), and 3.36(1) Å) indicate significant C−H···O hydrogen bonding,[4] which is presumably responsible for the ordering seen within the ethyl groups.

Figure 5c shows the ordered dabcoH$^+$ cation located inside the macrocycle, with its N···N vector significantly inclined to the general macrocyclic plane. It appears that the dabcoH$^+$ cation is simply too large to be accommodated inside the triangle in a manner that allows it to form an N−H···O hydrogen bond to one of the inner catechol oxygen centers; rather, the intra-triangle dabcoH$^+$ cation projects through the hole in the macrocycle so as to hydrogen bond to a water molecule on one side and to an *n*-propanol molecule on the other side. The intra-triangle dabcoH$^+$ cation participates in a number of C−H···O interactions (C···O, 3.279(7), 3.353(6), 3.391(7) Å) with oxygen atoms of the surrounding macrocycle. With the inclusion of the ordered intra-triangle dabcoH$^+$ cation, Figure 5c clearly shows the absence of 2-fold symmetry, however if one were to consider the anion in isolation, a pseudo 2-fold axis is apparent.

As a consequence of the spiro carbon atom, the two planar C_6O_2 units within the rigid L^{4-} ligand are at right angles to each other, and accordingly one may reasonably expect that the ligand is geometrically better suited to forming 4:4

(4) Desiraju, G. R. *Acc. Chem. Res.* **1996**, *29*, 441.

squares with four B^{3+} connectors than to forming 3:3 triangles with three B^{3+} connectors. As can be appreciated upon inspection of Supporting Information, Figure S1, the four boron centers in $[B_4L_4]^{4-}$ are close to, but somewhat "outside", the imaginary lines between the spiro carbon atoms that represent the "edge" of the square (spiro C···B···spiro C ~166°). In other words, the steric requirements of the rigid, angular L^{4-} components at the corners of the polygon impose some outward bowing upon the catechol-B-catechol edges even when the polygon is the 4:4 square; obviously, when the polygon is the 3:3 triangle this bowing will be more pronounced. All three triangle edges are inequivalent in the NEt_4^+ and dabcoH$^+$ derivatives, while the presence of the 2-fold axis in the other two derivatives means that two of the edges are equivalent and the third is different. As can be seen in Figure 5a, the two edges hydrogen bonded to the imidazolium cation are noticeably closer to linear (spiro C···B···spiro C angle, 150.8(2)°) than the third edge (spiro C···B···spiro C angle, 142.3(3)°). Likewise, as can be seen in Figure 2, the edge to which the Et_3NH^+ cation is hydrogen bonded (spiro C···B···spiro C angle, 151.1(2)°) is noticeably closer to linear than the other two edges (spiro C···B···spiro C angle, 147.5(1)°).

Solvated $(Et_4N)_3[B_3L_3]$ and $(dabcoH^+)_3[B_3L_3]$ crystallize in the triclinic space group $P\bar{1}$ whereas the solvated $(HNEt_3)_3[B_3L_3]$ and $(C_3H_5N_2)_3[B_3L_3]$ crystals adopt the monoclinic space group $C2/c$. Despite differences in crystal symmetry, the packing arrangements in all four compounds are similar.

All the extra-triangle $C_3H_5N_2^+$ cations are equivalent, both N−H units being used to bind one $[B_3L_3]^{3-}$ triangle to another by hydrogen bonds to catechol oxygen atoms (N···O, 2.716(7) Å), as can be seen in Supporting Information, Figure S2. The view down the stack, shown in Supporting Information, Figure S2a, reveals that all the cations are located inside the roughly rhombic prismatic envelope of the column, as was the case in $(Et_3NH)_3[B_3L_3]$. Consequently the columns in $(C_3H_5N_2)_3[B_3L_3]$ pack together in much the same way as those in $(Et_3NH)_3[B_3L_3]$, shown in Figure 4.

As indicated earlier, the Et_4N^+ crystals do not possess the 2-fold symmetry that is present in the $C_3H_5N_2^+$ and $HNEt_3^+$ crystals. This lack of symmetry is largely a consequence of the two distinct orientations adopted by the extra-triangle NEt_4^+ cations (Supporting Information, Figure S3). Nevertheless the column structure in $(Et_4N)_3[B_3L_3]$ (Supporting Information, Figure S3), is closely analogous to that in $(Et_3NH)_3[B_3L_3]$ and again the packing of the columns is similar.

The representations of $(dabcoH^+)_3[B_3L_3]$ presented in Figure 6 highlight the similarity of this packing with that found in the other structures described above. On closer inspection, however, it is clear that there are minor but nevertheless significant differences. First, the two types of enantiomeric triangles within a single column have been shifted relative to each other; in Figure 6 the gold triangles have been shifted downward while the blue triangles have been shifted upward compared with the stacks represented in Figure 3a and Supporting Information, Figures S2a and S3a. Second, while one type of extra-triangle cation lies clearly inside the column, part of the second type of cation lies just beyond the boundary of the prismatic column defined by the $B_3L_3^{3-}$ stacks. These differences make the absence of the 2-fold symmetry more pronounced than in the NEt_4^+ structure, which also has triclinic symmetry.

The structural features characteristic of the four compounds considered are columns of close to rhombic cross-section with an overall zero electrical charge which pack together in the same way; the cations are not involved in binding column to column, only in binding together the components within a column. Although the crystals described in this work fall into two distinct crystal classes, the similarity in the packing is reflected in a comparison of the reduced cells for the four compounds considered. Inspection of Table 2 reveals the reduced cells for all four compounds are similar.

Mass Spectrometric Studies. Electrospray mass spectrometry of the four compounds reveals a major peak in each case, corresponding to a dianion of composition $[(B_3L_3^{3-})(Cat^+)]$ ($Cat^+ = HNEt_3^+$, $C_3N_2H_5^+$, $HNEt_3^+$, and dabcoH$^+$). For each of the spectra the second most intense signal corresponds to the $B_3L_3^{3-}$ trianion (Table 3). The presence of the dianion as the major peak and the absence of a signal corresponding to a monoanion suggests that $[(B_3L_3^{3-})]$ interacts strongly with only a single cation. This is not surprising given that each of the crystal structures show a complementary electrostatic interaction between a trianionic macrocycle and a monocation of appropriate size and geometry.

Solution NMR Solution Studies. The ^{1}H NMR spectrum of each of the compounds is relatively simple. In each spectrum, single resonances are found for each of the two types of aromatic protons (6.25−6.30 and 5.52−5.62 ppm), the methyl protons (1.20−1.25 ppm), and each of the two types of methylene protons (1.90−1.93 and 2.21−2.25 ppm). These spectra indicate that the B_3L_3 triangle possesses D_3 symmetry in solution, at least on the NMR time scale, and that the cation appears to exert little influence on the chemical shifts of the triangle protons. Furthermore, for the cations in each compound, only a single set of resonances is found, indicating that if a cation were sitting inside the B_3L_3 triangle in solution that cation exchange was faster than the NMR time scale. For the purposes of comparison a ^{1}H NMR spectrum was collected on a sample of the square macrocycle $(B_4L_4)(NH_4)_4$. This spectrum indicated the macrocycle possessed D_4 symmetry but with resonances different from those of the triangles (aromatic protons: 6.25, 5.84 ppm; methyl protons: 1.26, 1.23 ppm; methylene protons: 2.22, 1.86 ppm).

In a wide variety of finite and infinite supramolecular systems the structure directing ability of hydrogen bonding interactions has been recognized as a powerful influence in the self-assembly process.[5] Although hydrogen bonding is apparent in some of the structures considered here, the

(5) Ward, M. D. *Chem Commun.* **2005**, 5838.

fact that similar structures are obtained, regardless of the extent of hydrogen bonding between the cations and anions, suggests that ionic interactions between the triangular anions and the intra- and extra- nitrogen-based cations are largely responsible for the packing arrangement within this novel series of structures. The incorporation of the cation within the macrocycle in the crystal structures of all four compounds not only provides an indication of a strong ionic interaction but suggests that the cation predisposes the components to assemble into a triangle rather than in some alternative manner. In the electrospray mass spectral analyses the dominance of the signal due to the macrocyclic $B_3L_3^{3-}$ anion with a single cation also provides support for a strong association between the anion and the internally bound cation.

Acknowledgment. We gratefully acknowledge the financial support of the Australian Research Council.

Supporting Information Available: Crystallographic data in CIF format, and Figures S1−S4. This material is available free of charge via the Internet at http://pubs.acs.org.

IC800544J